

The Gödel Engine - An interactive approach to visualization in general relativity

F. Grave^{1,2}, T. Müller¹, C. Dachsbacher¹ and G. Wunner²

¹Visualization Research Center, University of Stuttgart, Germany
²1. Institute for Theoretical Physics, University of Stuttgart, Germany

Abstract

We present a methodical new approach to visualize the aspects of general relativity from a self-centered perspective. We focus on the visualization of the Gödel universe, which is an exact solution to Einstein's field equations of general relativity. This model provides astounding features such as the existence of an optical horizon and the possibility of time travel. Although we know that our universe is not of Gödel type, we can – using this solution to Einstein's equations – visualize and understand the effects resulting from the theory of relativity, which itself has been verified on the large scale in numerous experiments over the last century. We derive the analytical solution to the geodesic equations of Gödel's universe for special initial conditions. Along with programmable graphics hardware we achieve a tremendous speedup for the visualization of general relativity. This enables us to interactively explore the physical aspects and optical effects of Gödel's universe. We also demonstrate how the analytical solution enables dynamic lighting with local illumination models. Our implementation is tailored for Gödel's universe and five orders of magnitude faster than previous approaches. It can be adapted to manifolds for which an analytical expression of the propagation of light is available.

Categories and Subject Descriptors (according to ACM CCS): I.3.7 [Computer Graphics]: Three-Dimensional Graphics and Realism —J.2 [Physical Sciences and Engineering]: Physics—G.1.7 [Numerical Analysis]: Ordinary Differential Equations —Initial value problems

1. Introduction

Albert Einstein has revealed the curved nature of space and time when he found the theory of general relativity. Kurt Gödel's universe is one of the most interesting exact solutions to Einstein's equations. Despite its mathematical simplicity, due to the high symmetry of the underlying spacetime, it demonstrates the possibilities lying within the theory of general relativity. Gödel's model of an alternative universe – only consisting of homogeneous dust, rotating around every point – describes a theoretically feasible spacetime, in which time travel is possible beyond an optical horizon, which itself represents a non-impenetrable physical barrier for massive particles.

In this paper we visualize optical effects of general relativity from a first person's point of view. This is done by placing an observer in a specific general relativistic model such as the Gödel universe. Our goal is to render an image of the observer's view in such spacetimes and allow for inter-

active movement of objects, light sources, and the observer camera. In this work, we focus on the geometrical appearance and local illumination of objects in Gödel's universe and neglect relativistic effects such as frequency shifts due to relative motion. In prior implementations, the geodesic equations which describe the propagation of light are integrated numerically to determine the curved rays on which light travels. The resulting segments are then used for intersection calculations similar to standard raytracing for finding the direction from which a certain object is seen. This procedure is very costly and the resulting images lack illumination as the incident light direction is indeterminable due to the geodesics. The straightforward implementation of an analytical solution to the geodesic equations to generate these segments decreases rendering time drastically, but still does not result in interactive frame rates.

Our approach avoids a numerical integration and directly computes the locations where an object is visible. This re-

quires an analytical solution to the geodesic equations which we derive for Gödel's universe. We can interactively alter the visualization parameters and discover effects which are hardly possible to find with non-interactive methods. Exploiting the analytical solution it is also possible to apply a local illumination model. We chose Gödel's universe for our visualization due to its elegant mathematical structure and physical implications. Please note that recent solutions to the geodesic equations of other spacetimes such as wormholes can be used as well.

The remainder of this paper is structured as follows. In Sect. 3 we provide a short outline of general relativity and the basic physical properties of Gödel's universe. We also discuss the optical appearance of objects in Gödel's universe by investigating the characteristics of light rays. The method and shortcomings of four-dimensional raytracing on curved manifolds are discussed in Sect. 4. Next, our solution to the geodesic equations for special initial conditions will be outlined and processed in Sect. 5.1 and 5.2. To enable arbitrary observer positions as well as local illumination models, we take the symmetries of Gödel's universe into account in Sect. 5.3. The implementation and applications of our approach are discussed in the last section.

2. Related work

Weiskopf [Wei01] visualized many visual properties of relativity using a four-dimensional extension to the raytracing system RayVIS [Gro96]. Müller [Mü06] extended this idea further when implementing a formulation of objects with respect to their local flat frame of reference. In recent years several relativistic scenarios were implemented in interactive simulations utilizing modern graphics hardware. Like the work of Savage et al. [SSM07] these implementations are restricted to special relativistic scenarios where light paths resemble straight lines. Müller [Mü08] has provided interactive visualizations of general relativistic wormholes using an analytical solution, with limitations, however, such as ambient lighting. In our previous work [GB08] we introduced a generic approach to visualizing various spacetimes faster by means of a slow preprocessing step and an interactive post-processing method to alter certain parameters of a scene. It is, however, not possible to move objects unless another preprocessing step is done. Also, the concept of a noninteractive local illumination model exploiting the symmetries of spacetime – in our case the Gödel universe as well – has been introduced.

There exist numerous publications on the solution to the geodesic equations of Gödel's universe, most prominent being the work of Kundt [Kun56], Chandrasekhar et al. [CW61] and Novello et al. [NST83]. Kajari et al. [KWS04] found a very convenient set of coordinates, in which Gödel's universe reveals its properties more apparent. Also, the symmetries of Gödel's universe were provided, alongside a special solution to the geodesic equations. In

contrast to our solution, Kajari. et al. restricts the solution to the $\{t, r, \varphi\}$ -subspace and therefore neglect the z -coordinate of Gödel's universe.

All visualizations of general relativity – interactive, semi-interactive or non-interactive – restrict themselves to visualize primitive objects such as spheres or cubes. Gu et al. [GGH02] provided an efficient way to store mesh data in geometry images. This idea, as well as recent techniques in programmable graphics hardware such as CUDA [NVI] and the method of texture space lighting [BJ03], were adopted in this work to enable rendering of arbitrary geometry.

3. Theory of general relativity and the Gödel universe

In this section we provide a brief introduction to the concepts of general relativity and the Gödel universe. An in-depth discussion on relativity can be found in [Rin01, MTW73] while details on the Gödel universe are illustrated in [KWS04].

3.1. Basic characteristics of general relativity

Einstein found that the three spatial dimensions and time itself cannot be described as separate entities but form a four-dimensional spacetime continuum. From a mathematical point of view, these spacetimes are represented by four-dimensional pseudo-Riemannian manifolds, which are solutions to Einstein's field equations. Einstein also discovered that these manifolds are curved if masses are present in a particular spacetime. This curvature is implied in the line element $ds^2 = \sum_{\mu, \nu=0}^3 g_{\mu\nu}(\mathbf{x}) dx^\mu dx^\nu$, which characterizes any spacetime in general relativity. Here $g_{\mu\nu}(\mathbf{x})$ is the metric tensor at the point \mathbf{x} , and is the diagonal matrix $\text{diag}(-1, 1, 1, 1)$, if the underlying manifold is flat and cartesian coordinates are used. For a given set of coordinates x^μ there is a unique metric tensor $g_{\mu\nu}$ (except for the algebraic sign). The line element ds measures the spacetime distance between two infinitesimally neighboring events \mathbf{x} and $\mathbf{x} + d\mathbf{x}$, where dx^μ expresses the infinitesimal coordinate difference along the μ -axis of the coordinate system. From this line element, many physical features considered in general relativity can be extracted considering a particular spacetime. For example, using the Christoffel symbols the so called geodesic equations

$$\ddot{x}^\sigma + \sum_{\mu, \nu=0}^3 (\Gamma_{\mu\nu}^\sigma \dot{x}^\mu \dot{x}^\nu) = 0 \quad (1)$$

with the constraint $g_{\mu\nu} \dot{x}^\mu \dot{x}^\nu = \kappa c^2$ can be derived. The differentiation $\dot{x}^\mu = \partial x^\mu / \partial \lambda$ is with respect to the curve parameter λ . The four geodesic equations describe how photons ($\kappa = 0$) or massive particles ($\kappa = -1$) propagate when they are solely under the influence of gravitation. The affine curve parameter λ is the proper time of the particle if $\kappa = -1$. For photons the curve parameter has no physical meaning. The geodesic equations are second-order differential equations, they can be solved by formulating an initial-value problem

for a particular spacetime point \mathbf{x}_s and direction $\hat{\mathbf{x}}_s$. Unfortunately the geodesic equations are usually very hard to solve analytically. However, for various spacetimes an analytical solution was found.

3.2. Gödel's solution

Kurt Gödel, who was a close friend of Albert Einstein, was fascinated by general relativity. He soon discovered that this theory does not necessitate a global time order and therefore allows time travel. Gödel tried to find a solution to Einstein's field equations with this property [SF90] and succeeded in discovering a world model later named after him. The line element in Gödel's universe [KWSD04] is

$$ds^2 = -c^2 dt^2 + \frac{dr^2}{1 + [r/(2a)]^2} + r^2 (1 - [r/(2a)]^2) d\varphi^2 + dz^2 - \frac{2r^2 c}{\sqrt{2a}} dt d\varphi, \quad (2)$$

with cylindrical coordinates $\{r, \varphi, z\}$, the time coordinate t , the velocity of light c , the Gödel parameter a , and the convention $g_{00} < 0$. It can be shown [Gö49] that this solution describes a homogeneous, but rotating and therefore not isotropic, universe. Due to the homogeneity of Gödel's universe there is no gravitational redshift, only Doppler shift due to relative motion arises. The mass distribution generating the curvature of Gödel's universe consists of dust, which is rigidly rotating around every point. The angular velocity of this rotation is inversely proportional to the Gödel parameter a . This set of coordinates is very intuitive compared to other formulations, such as [Gö49, Pfa81]. In the limit $a \rightarrow \infty$ this spacetime yields the nonrotating flat spacetime of special relativity in cylindrical coordinates. Therefore, a specific situation, e.g. a certain arrangement of objects, can be designed in flat spacetime before introducing rotation ($a = a_0$) to this model.

It can be shown [Kun56, CW61] that time travel is in fact possible in Gödel's universe. A person – starting at the origin and traveling beyond the Gödel horizon and back – can travel into the past of an observer remaining located at the origin of this coordinate system. This does *not* mean that the time traveler himself gets younger as he travels into the past of the resting observer. An older duplicate of the traveler returns to the origin before the younger version of himself even leaves. The philosophical consequences concerning causality are – to say the least – severe, but this kind of travel is possible within the Gödel universe. Furthermore, as this model is not the only spacetime allowing time travel [Pfa81] it must be concluded that time travel is an immanent characteristic of general relativity.

As the Gödel universe is a valid solution to Einstein's field equations, it is a *possible* description of our universe. On the other hand we know that the Gödel universe is no realistic description of our universe because the Gödel metric describes a rotating, not expanding universe, whereas our

universe is not rotating but expanding. Nevertheless, this solution demonstrates that time travel is in principle possible if we only take general relativity into account. Most physicists including Einstein himself stated that time travel should be impossible due to the resulting severe causality violations, but there is obviously no mechanism within the domain of general relativity itself preventing time travels.

3.3. Optical appearance of Gödel's universe

In Fig. 1, the curved paths of light rays starting at the origin are depicted. The black geodesics and the rotational symmetry show that there exists a maximum radial distance which photons reach if they have passed through the origin. This Gödel horizon is a cylinder around the z -axis with radius $r_G = 2a$. It is the maximum distance that an object can reach before it disappears for an observer located at the origin. Consequently, the Gödel horizon is an optical horizon but it can be shown that it is no physical barrier which objects could not penetrate. Objects beyond the Gödel horizon are simply not visible from the origin of this coordinate system. If an object is located within the Gödel horizon it will be visible at least twice as illustrated in Fig. 1: There exist two possible paths for light to travel from an object to the observer located at the origin.

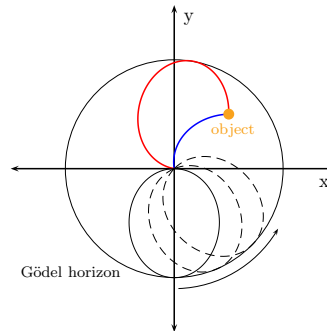


Figure 1: Geodesics in the xy -plane. Example geodesics (black) and the rotational symmetry of the spacetime illustrate the existence of an optical horizon. An object (orange) can be seen twice.

By pushing the object to a position with $z \neq 0$ within the horizon, it will be visible infinitely often (Fig. 2): There exists an infinite number of increasingly narrow helix-like paths, which connect the object to the observer. Fig. 3 shows an example rendering of a small object located above the xy -plane and within the Gödel horizon. We denote a physical entity within the Gödel universe an *object* and the multitude of its visible appearances *representations*.

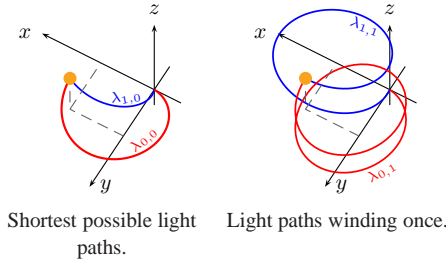


Figure 2: Light paths from a small object (orange) to an observer located at the origin. An infinite number of possible light paths exists with any number of windings. The variables $\lambda_{i,j}$ serve to distinguish the different geodesics and will be properly introduced in Sect. 5.2.



Figure 3: Optical appearance of an infinitely often visible sphere (only a finite number of representations shown) located within the Gödel horizon ($z > 0$).

4. Visualization of general relativity

4.1. From 3D raytracing to general relativistic 4D raytracing

In classical 3D raytracing a primary ray is cast from the camera into the scenery and intersections between the ray and objects are calculated. Secondary rays are generated at these intersection points which connect them to light sources to apply local illumination models. All light contributions are accumulated to determine the final color of a surface point hit by a primary ray. To take the velocity of light into account a fourth dimension has to be introduced into the rendering process which stores the time that light needs to travel and the information on when the camera or an object reaches a certain position. By implementing the Lorentz-transformation [Rin01] between frames of reference in relative motion, effects of special relativity can be visualized.

In general relativity paths of light, as well as massive particles, are determined by the geodesic equations (Eq. 1) and are generally curved. If no solution to these equations for a particular spacetime is known they have to be integrated numerically using standard methods such as Runge-Kutta integrators. The resulting paths are approximated with linear segments which can then be used to calculate intersections between a primary ray originating from a camera and the objects in the scenery which can both be moving. A detailed discussion on general relativistic raytracing can be found in [Wei01, Mü06].

4.2. Shortcomings in 4D raytracing

There are two main problems in general relativistic raytracing. First, the numerical integration of geodesics on today's standard CPUs usually takes about ten milliseconds per ray. The calculation of intersections between this ray and a single object requires another millisecond. The amount of time for rendering a large image of a complex scenery easily exceeds a whole day even if a cluster is used. Second, if no analytical solution is available, the relativistic rendering cannot integrate lighting computations. The inherent problem is that it is basically impossible to connect two spacetime points with curved rays using an initial value problem. Simply speaking, we do not know the direction in which a secondary ray has to start to reach the light source if this ray is bent arbitrarily. For interactive visualizations we either need extraordinary powerful clusters for integrating geodesics and intersection computation or an analytical solution to the geodesic equations which we present in the following section.

5. The geodesics and symmetries of Gödel's universe

5.1. Solution to the geodesic equation

The analytical integration of the geodesic equations can be an impossible or at best tedious task. However, due to the large number of symmetries and the resulting constants of motion we can solve the geodesic equations for the Gödel universe. In this section, we present the solution to the geodesic equations (Eq. 1) for special initial conditions. We outline the solution – the full derivation in detail goes beyond the scope of this work. The Lagrangian formalism is used to derive the solutions. For the mathematical details we refer the interested reader to [MTW73].

The Lagrangian for photons

$$\mathcal{L}(\mathbf{x}, \dot{\mathbf{x}}) = \sum_{\mu, \nu=0}^3 g_{\mu\nu} \dot{x}^\mu \dot{x}^\nu \stackrel{!}{=} 0$$

is independent of t, φ and z , because the metric tensor itself does not depend on these coordinates. From the Euler-Lagrange equations of motion

$$\frac{d}{d\lambda} \frac{\partial \mathcal{L}}{\partial \dot{x}^\mu} - \frac{\partial \mathcal{L}}{\partial x^\mu} = 0,$$

we obtain three constants of motion for t, φ and z by applying the Noether theorem

$$k_i := \frac{\partial \mathcal{L}}{\partial \dot{x}^i}, \text{ where } i = 0, 2, 3.$$

These constants of motion can then be used to decouple the radial equation of motion ($i = 1$) from the other equations. With this step we obtain four ordinary differential equations where the time and the angular equation are coupled with the radial equation. These equations can be considerably simplified when restricting the solution process to the special initial condition $x_s^1 = r_s = 0$, where k_2 vanishes and k_0 only contains the time direction.

The radial equation can be solved, yielding the solution $r(\lambda)$, which is inserted into the other equations. These can then be integrated. All four integrals of the equations of motion can be found in standard integration tables, e.g. [BSMM07]. The result of this derivation in geometrical units ($c = 1$) is:

$$t(\lambda) = k_0\lambda - 2\sqrt{2}ak_0g(\lambda) + f_{1/2}(\lambda), \quad (3a)$$

$$r(\lambda) = 2a\sqrt{\frac{1-k_3^2}{1+k_3^2}} \left| \sin\left(\frac{\sqrt{1+k_3^2}}{2a}\lambda\right) \right|, \quad (3b)$$

$$\varphi(\lambda) = -k_0g(\lambda) + f_{1/2}(\lambda) - f_0(\lambda) + \varphi_s, \quad (3c)$$

$$z(\lambda) = k_3\lambda, \quad (3d)$$

with

$$f_q(\lambda) = \pi \left\lfloor \frac{\sqrt{1+k_3^2}}{2a\pi}\lambda + q \right\rfloor, \quad (4a)$$

$$g(\lambda) = \arctan\left(\frac{\sqrt{2}}{\sqrt{1+k_3^2}} \tan\left(\frac{\sqrt{1+k_3^2}}{2a}\lambda\right)\right). \quad (4b)$$

The function $\lfloor x \rfloor$ returns the largest integer smaller than x , k_0 is the negative time direction (e.g. +1 for light traced into the past), and $\vartheta_0 = \arccos(k_3)$ as well as φ_0 are related to the starting direction of the light particle as illustrated in Fig. 4.

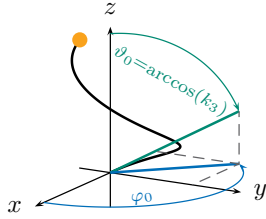


Figure 4: The starting direction of the geodesic is formulated with respect to the angular coordinates ϑ and φ of a spherical coordinate set.

5.2. Processing the solution of the geodesic equations

Fig. 4 shows the resulting geodesic reaching a certain point (orange) for a given set of initial values. For a fast visualization technique the question has to be reversed: What are the sets of initial conditions such that resulting geodesics connect a given point to the origin? To find all geodesics which connect the origin to an arbitrary static point $\mathbf{x}_p = (t_p, r_p, \varphi_p, z_p)$ the equations

$$x^\mu(\lambda) = x_p^\mu \quad (5)$$

have to be solved, where the left-hand side corresponds to the analytical solution (Eq. 3) and the right-hand side is the

point \mathbf{x}_p . The radial equation in $\mu = 1$ reads

$$\left| \sin\left(\frac{1+k_3^2}{2a}\lambda\right) \right| = \frac{r_p}{2a} \sqrt{\frac{1+k_3^2}{1-k_3^2}}$$

and yields the solutions

$$\lambda_{0,n} = \frac{2a}{\sqrt{1+k_3^2}} [h_a(k_3) + n\pi], \quad (6a)$$

$$\lambda_{1,n} = \frac{2a}{\sqrt{1+k_3^2}} [-h_a(k_3) + (n+1)\pi]. \quad (6b)$$

where

$$h_a(k_3) = \arcsin\left(\frac{r_p}{2a} \sqrt{\frac{1+k_3^2}{1-k_3^2}}\right) \quad (7)$$

The first index in $\lambda_{i,j}$ denotes whether the geodesic is on the outbound part of the geodesic ($i = 0$) or on the incoming part which has already reached the horizon ($i = 1$) within this cycle. The second index j is the number of full cycles that the geodesic has run through since starting from the origin. This is the notation also used in Fig. 2. The unknown parameter k_3 is determined by Eq. 3d, in which Eqns. 6a and 6b are inserted. Unfortunately, the resulting equations

$$\frac{k_3}{\sqrt{1+k_3^2}} [h_a(k_3) + n\pi] = \frac{z_p}{2a}, \quad (8a)$$

$$\frac{k_3}{\sqrt{1+k_3^2}} [-h_a(k_3) + (n+1)\pi] = \frac{z_p}{2a}, \quad (8b)$$

cannot be solved analytically and thus these two equations have to be handled numerically using, e.g., a regula falsi method. However, the numerical effort is negligible compared to the numerical integration of geodesics.

Having obtained the solutions to these equations – a set of parameters $\{k_3\}$ for the different possible geodesics – we know the vertical angles $\{\vartheta_{i,j}\}$ under which the object is visible using $\vartheta_0 = \arccos(k_3)$ (Fig. 4). The horizontal angles $\{\varphi_{i,j}\}$ can be obtained using Eq. 3c and $\lambda_{i,j} = 0$. By this calculation we find a set of initial conditions for geodesics connecting a visible point to the origin. We can now calculate the directions in the three-dimensional subspace at the observer's position under which all representations of this point can be seen. A correct occlusion of object's instances is achieved by considering the geodesics' relative lengths given by $\lambda_{i,j}$. The direction and final position of each representation is then given by

$$\vec{\mathbf{v}}_{i,j} = \begin{pmatrix} \sin(\vartheta_{i,j}) \cos(\varphi_{i,j}) \\ \sin(\vartheta_{i,j}) \sin(\varphi_{i,j}) \\ \cos(\vartheta_{i,j}) \end{pmatrix}, \quad \vec{\mathbf{x}}_{i,j} = \lambda_{i,j} \vec{\mathbf{v}}_{i,j}. \quad (9)$$

The orange object in Fig. 4 can therefore be seen along the direction of the green line. As a point is infinitely often visible we create a (finite) number of copies of it. Following this procedure we generate a scene with multiple instances of

each object. If an object is partially beyond the Gödel horizon, the last visible vertices of the two representations $\{0, j\}$ and $\{1, j\}$ on the same helix winding are contracted using a stitching algorithm. Now this scene can be rendered using a standard perspective camera.

In addition to an observer at the origin we can also place a point light source there in order to illuminate the object. The use of a local illumination model is then possible, because we can compute if and how the origin is connected to an arbitrary point. The only difference is the time direction in which the geodesics are traced. For calculating the position of an object geodesics are traced back into the past. The illumination of an object requires geodesics propagating into the future instead.

Using this derivation we can avoid an expensive numerical integration of geodesics and tedious intersection calculations. Note, however, that it is still not possible to obtain visualizations for arbitrary positions of both observer and point light. Although the analytical solution to arbitrary initial conditions exists, it can be shown that this solution is too complex for an interactive visualization.

5.3. Using isometries to avoid rendering restrictions

Symmetries of a problem allow one to transform a given coordinate set to another more convenient set of coordinates easily, in which the properties of the underlying model become clearer. For example consider the analysis of the characteristics of two particles rotating around each other due to the influence of classical Newtonian gravity: A reasonable choice is a rotating polar coordinate system with its origin located at the center of mass. The idea of choosing an appropriate set of coordinates is also employed in computer graphics when transforming camera or object positions. This concept can be used in general relativity through isometries. An isometric transformation ξ^α is an infinitesimal coordinate transformation

$$x'^\alpha(\eta) = x^\alpha + \eta \xi^\alpha(x^\beta) \quad (10)$$

with $\eta \ll 1$. By definition, the metric tensor remains unchanged under this transformation. In mathematical terms an isometry is represented by a Killing vector field [MTW73]. It determines the directions in which the infinitesimal transformation has to be undertaken in order to retain the metric and thus the physics of the spacetime described. To obtain a finite isometric transformation Eq. 10 is differentiated with respect to η to obtain the differential equation

$$\frac{dx^\alpha(\eta)}{d\eta} = \xi^\alpha(x^\beta). \quad (11)$$

The solution to this equation resembles an isometric transformation along $\xi^\alpha(x^\beta)$ for finite values of η . Gödel's universe inherits five independent isometries [KWSD04] which can be linearly combined to form another Killing vector

field: ξ_a^α is a translation in time, ξ_b^α a rotation around the z -axis, ξ_c^α a translation along the z -axis, ξ_d^α a translation along $\zeta^\alpha(r, \varphi)$, and ξ_e^α along $\zeta^\alpha(r, \varphi - \frac{\pi}{2})$. Being dependent on both r and φ , ζ^α is given by

$$\begin{pmatrix} \zeta^0 \\ \zeta^1 \\ \zeta^2 \\ \zeta^3 \end{pmatrix} = \frac{1}{\sqrt{1 + [r/(2a)]^2}} \begin{pmatrix} \frac{r}{\sqrt{2c}} \cos \varphi \\ a \left[1 + \left(\frac{r}{2a}\right)^2 \right] \sin \varphi \\ \frac{a}{r} \left[1 + 2 \left(\frac{r}{2a}\right)^2 \right] \cos \varphi \\ 0 \end{pmatrix}.$$

However, for $\phi = \pm\pi/2$ the vector ζ^α points along the radial axis of the coordinate system making it a mere radial translation dr . The resulting differential equation to Eq. 11 can easily be solved analytically in the same way. This can be used for the following train of thoughts: Take an observer position in the xy -plane and a collection of objects in the Gödel universe. If the observer was located at the origin a fast visualization of this scene is possible using the derivation of Sect. 5.2. Using a concatenation of isometric transformations it is possible to transform the whole scenery such that the observer is located at the origin of the new coordinate system. Fig. 5 depicts the concatenation of two suitable isometric transformations. First, the observer's position (yellow) is rotated around the origin along the rotational Killing vector field ξ_1^α onto the y -axis of the coordinate system. The gray object is rotated by the same angle η_1 . In a second step, the observer's location is transformed along the field $-\xi_3$ to the origin. Again, the gray object is transformed with the same curve parameter η_3 . Note that the latter transformation is *not* a solely radial translation if the transformed object is located at an arbitrary position. The generalization of an arbitrary observer position with $z \neq 0$ is simple, because the isometry ξ_2^α is a translation parallel to the z -axis. Following

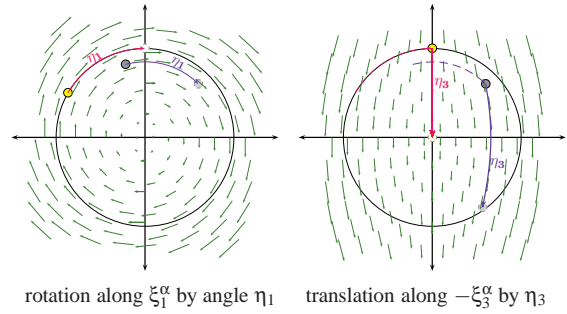


Figure 5: Concatenation of isometric transformations. The yellow object denotes an observer or a light source, the gray object resembles an arbitrary visualized object.

these ideas it is also possible to apply arbitrary point light sources. Instead of transforming the observer's position to the origin of the coordinate system the light source is moved. Being able to connect origin and arbitrary spacetime points it is directly possible to calculate whether or not a certain position is illuminated.

6. Implementation

Our implementation resembles the derivation presented in Sec. 5. In Sec. 5.2 we discussed how to calculate the directions under which a single point in Gödel's universe is seen from the origin using the analytical solution derived in Sec. 5.1. In a practical implementation which renders images from triangle meshes these computations are carried out per vertex to facilitate efficient triangle rendering. We first recapitulate the vertex transformation, followed by details on the *OpenGL* and *CUDA* implementation. For the transformation only Eqns. 8 have to be solved numerically which is achieved using the Illinois-method, a modified regula falsi procedure, converging typically in less than ten iterations. Eq. 9 then gives us the direction under which a surface point, or vertex, is visible on the image plane.

To enable arbitrary observer positions we use the concept of finite isometric transformations illustrated in Sec. 5.3. The observer position is isometrically translated into the origin and each vertex is transformed analogously (Fig. 5). A vertex is transformed numerically using a standard 4th-order Runge-Kutta integrator, while the observer position is transformed using an easily obtainable special solution to Eq. 11. Next, the view directions for each vertex are calculated using the special solution to the geodesic equations as recapitulated above. Since light travels from the objects to the observer the primary rays – cast into the opposite direction – travel into the past, i.e. $k_0 = +1$ for Eqns. 3. The analytical solution also allows us to apply local illumination models. For this the light source is translated isometrically into the origin and we then illuminate the vertices by finding the geodesics reaching the surfaces; these geodesics propagate into the future and here $k_0 = -1$.

We assume objects to be small and solve the isometric transport equation (Eq. 11) for the center point of an object only. This is physically reasonable as objects are formulated with respect to their local flat frame of reference located at a certain point on the manifold, which has also been used as the center point of the object [Mü06]. The numerical solution to the isometric transport equation is implemented on the CPU as it is required only once per frame and object.

In our implementation we use geometry images as representation for our triangle meshes which we store in vertex buffer objects (VBO). Note that geometry images exhibit an implicit topology where 2×2 neighboring pixels form two triangles. In addition to the geometry images storing vertex positions and normals we create an additional VBO storing illumination values per vertex. Since we carry out all computations on vertices stored in VBOs we opted for an implementation using *CUDA* [NVI]. The mesh VBOs containing the input vertex positions, texture coordinates and normals of the meshes are accessible in *CUDA* and remain unchanged throughout the rendering passes.

Note that every object can be seen infinitely often in Gödel's universe. We account for this by rendering a finite

number of pairs of instances, e.g. the two top-most spheres in Fig. 3, corresponding to occurrences seen under geodesics with the same number of windings (see Fig. 2). The rendering of one pair consists of the following steps: First we accumulate the contribution from all light sources into the lighting VBOs by applying the respective isometric transformation and computing the direct illumination. Note that this is very similar to texture space lighting techniques [BJ03]. Next we compute the solution to Eq. 8 for every vertex giving us the three-dimensional coordinate for display (Eq. 9). Vertices may be located beyond the Gödel horizon resulting in triangles that have to be excluded from rendering. Instead the pairwise instances have to be stitched together. For this we mark vertices in the geometry images which belong to valid and invalid triangles at the same time. Texels in the geometry images corresponding to these vertices are the same for both instances and we weld the vertices together by simply averaging their coordinates. As a result the two instances smoothly fuse as shown in Fig. 3.

The output of the *CUDA* computation can be mapped to *float*-arrays for the *OpenGL* pipeline by utilizing the *OpenGL*-interoperability. One VBO contains the solution of Eq. 8 for every vertex (possibly modified due to stitching), and a second VBO stores the illumination of every vertex in the geometry images. We render the image as seen from the observer by using *GLSL* shaders and depth buffering to resolve occlusions. Correct depth sorting is achieved by using λ as monotonic measure for relative distance (Eq. 9) while using the same depth buffer across all passes.

7. Results

The direct comparison between a standard raytracing approach and our implementation reveals a drastic difference in performance. A reference scene containing one object has been rendered using both methods on a standard dual-core desktop PC in a resolution of 1024x512 pixels. The raytracing approach to which we compare [Mü06] does not use supersampling, thus we rendered the images from the Gödel engine with no antialiasing or other image quality improving methods. Also, the local illumination model was deactivated, because no CPU implementation was available.

n	CPU A	CPU B	GPU	speed-up $\times 10^5$
2	41 s	605 s	4.1 ms	0.9 to 1.5
4	79 s	1105 s	7.8 ms	0.9 to 1.4
6	113 s	1639 s	11.2 ms	0.9 to 1.5

In the table above, the first column denotes the number of visualized representations. CPU A is a raytracing approach which implements the analytical solution. CPU B also is raytracing approach but uses a 4th order Runge-Kutta integration for the geodesic equations. We chose the integration parameters to match the image quality of our interactive approach. The GPU rendering time was measured on a GeForce 8800 GTS. Although a GPU implementation of a

numerical integrator is possible, no better performance compared to the analytical approach is to be expected.

With an average performance gain of five orders of magnitude, our approach enables us to visualize effects such as a local illumination model. We consider the correct angular dependency between reflected secondary ray and the direction under which the primary ray intersects the object. With 16xMSAA and more complex objects and scenarios the rendering time increases to non-interactive rates but still remains under a second for a reasonable size of the scene.

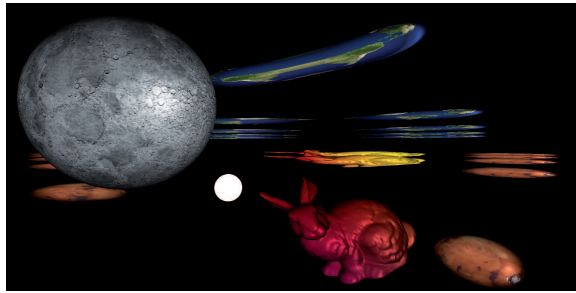


Figure 6: High quality image of multiply appearing objects and a point light source (white) rendered in 730 ms.

8. Conclusion

We have achieved a performance leap of five magnitudes. This enables us to discover astounding optical features of Gödel's universe. The accompanying video clearly reveals these effects: An object can disappear behind the Gödel horizon before being occluded by a higher order representation of another object. Another example is the quasistatically moving point light source. Although it disappears behind the Gödel horizon, its reflections can still be seen. These effects might not have been discovered without an interactive approach.

To find such amazing features it is mandatory to be able to "play" with visualization parameters and obtain the results as fast as possible. The extension of our idea to other manifolds where analytical expressions on curved light rays are available is possible, thus to supporting research in other fields. Taking our application itself to a general audience can improve their understanding of relativistic effects.

9. Future work

Our results reveal a tremendous speedup of five orders of magnitude, but we strive to further increase rendering speed. In our current method we consider static or slow moving objects. To be able to correctly visualize fast moving objects we have to take the velocity of light into account. This is also crucial when correctly visualizing time traveling objects where it is important to know the exact time when a photon perceived was emitted. An interactive implementation along with shadow rendering and distance attenuation appears possible and is subject to future work.

Acknowledgements: The authors wish to thank Sebastian Grottel, Christoph Müller, Katrin Bidmon, Michael Buser and Tom Ertl for many fruitful discussions. We also thank the Deutsche Forschungsgemeinschaft (DFG) for funding this work (project number: 99015432).

References

- [BJ03] BORSHUKOV G., J.P.LEWIS: Realistic human face rendering for "The Matrix Reloaded". *International Conference on Computer Graphics and Interactive Techniques, ACM SIGGRAPH 2003 Sketches & Applications* (2003).
- [BSMM07] BRONSTEIN I., SEMENDJAJEW K., MUSIOL G., MÜHLIG H.: *Handbook of Mathematics*. Springer, 2007.
- [CW61] CHANDRASEKHAR S., WRIGHT J. P.: The Geodesics in Gödel's Universe. *Proc. Natl. Acad. Sci. U.S.A* (1961), 341–347.
- [GB08] GRAVE F., BUSER M.: Visiting the Gödel Universe. *IEEE Transactions on Visualization and Computer Graphics* 14, 6 (November/December 2008), 1563–1570.
- [GGH02] GU X., GORTLER S., HOPPE H.: Geometry images. *ACM SIGGRAPH 2002 Conference Proceedings* (2002), 355–361.
- [Gro96] GROENE A.: *Entwurf eines objektorientierten Visualisierungssystems auf der Basis von Raytracing*. PhD thesis, Eberhard-Karls-Universität Tübingen, 1996.
- [Gö49] GÖDEL K.: An Example of a New Type of Cosmological Solutions of Einstein's Field Equations of Gravitation. *Reviews of Modern Physics* 21, 3 (July 1949), 447–450.
- [Kun56] KUNDT W.: Trägheitsbahnen in einem von Gödel angegebenen kosmologischen Modell. *Z. Phys.* 145 (1956), 611–620.
- [KWSD04] KAJARI E., WALSER R., SCHLEICH W. P., DELGADO A.: Sagnac Effect of Gödel's Universe. *Gen. Rel. Grav.*, 36 (2004), 2289–2316.
- [MTW73] MISNER C. W., THORNE K. S., WHEELER J. A.: *Gravitation*. W. H. Freeman, 1973.
- [Mü06] MÜLLER T.: *Visualisierung in der Allgemeinen Relativitätstheorie*. PhD thesis, Eberhard-Karls-Universität Tübingen, 2006.
- [Mü08] MÜLLER T.: Exact geometric optics in a Morris-Thorne wormhole spacetime. *Phys. Rev. D* 77, 044043 (2008).
- [NST83] NOVELLO M., SOARES I. D., TIOMNO J.: Geodesic motion and confinement in Gödel's universe. *Phys. Rev. D* 27, 4 (1983), 779–788.
- [NVI] NVIDIA: CUDA Zone – The resource for cuda developers. Website. Available online at www.nvidia.com/cuda.
- [Pfa81] PFARR J.: Time Travel in Gödel's Space. *Gen. Rel. Grav* 13, 11 (1981), 1073–1091.
- [Rin01] RINDLER W.: *Relativity - Special, General and Cosmology*. Oxford University Press, 2001.
- [SF90] SOLOMON FEFERMAN E. A. (Ed.): *A Remark about the Relationship between Relativity Theory and Idealistic Philosophy, in Kurt Gödel: Collected Works, Vol. II*. Oxford University Press, 1990.
- [SSM07] SAVAGE C. M., SEARLE A., MCCALMAN L.: Real Time Relativity: Exploratory learning of special relativity. *Am. J. Phys* 75, 9 (Sept. 2007).
- [Wei01] WEISKOPF D.: *Visualization of Four-Dimensional Spacetimes*. PhD thesis, Eberhard-Karls-Universität Tübingen, 2001.